

## Nanostructures in silicon carbide crystals and films

S. I. Vlaskina

*Yeoju Institute of Technology (Yeoju University),  
338 Sejong-ro, Yeoju-eup, Yeoju-gun, Gyeonggi-do, 469-705 Korea*

*V. Lashkaryov Institute of Semiconductor Physics,  
National Academy of Science of Ukraine,  
45, Nauky Prosp., Kyiv 03028, Ukraine  
businkaa@mail.ru*

S. P. Kruchinin

*Bogolyubov Institute for Theoretical Physics,  
National Academy of Science of Ukraine, Kiev 03680, Ukraine  
skruchin@i.com.ua*

E. Ya. Kuznetsova

*National Aviation University, Kiev, Ukraine*

V. E. Rodionov

*V. Lashkaryov Institute of Semiconductor Physics,  
National Academy of Science of Ukraine,  
45, Nauky Prosp., Kyiv 03028, Ukraine  
rodionov@ukr.net*

G. N. Mishinova

*Taras Shevchenko Kyiv National University,  
64, Volodymyrs'ka Str., 01033 Kyiv, Ukraine*

G. S. Svechnikov

*V. Lashkaryov Institute of Semiconductor Physics,  
National Academy of Science of Ukraine,  
45, Nauky Prosp., Kyiv 03028, Ukraine*

Accepted 29 February 2016

Published 31 March 2016

Phase transformations of SiC crystals with grown original defects and thin films have been presented. The SiC crystals were grown by the Tairov method and the films were obtained by the “sandwich” and Chemical Vapor Deposition (CVD) methods.

The analysis of absorption spectra, excitation spectra and low-temperature photoluminescence spectra testifies to the formation of a new microphase during the growth.

The complex spectrum can be decomposed into similar structure-constituting spectra shifted on the energy scale relative to the former. Such spectra are indicators of the formation of new nanophases.

The joint consideration of photoluminescence spectra, excitement photoluminescence spectra and absorption spectra testifies to the uniformity of different spectra and the autonomy of each of them. Structurally, the total complexity spectra correlate with the degree of disorder (imperfection) of the crystal and are related to the peculiarities of a defective performance such as a one-dimensional disorder. Three different types of spectra have three different principles of construction and behavior.

*Keywords:* Nanostructures; films; phase transition.

PACS numbers: 73.63.Kv, 85.35.Be

## 1. Introduction

Correlations between the crystal structure and the optical properties (photoluminescence, absorption) are under discussion for polytypic materials. Silicon carbide polytypes are the best choice for such investigations. The actual atomic structures, accompanying lattice vibrations and the properties of layered combinations of polytypes can be considered with regard for the optical spectra.

In this work, we report on the phase transformations of SiC crystals and thin films with in-grown original defects. SiC crystals were grown by the Tairov method and films were obtained by the “sandwich” methods and by chemical vapor deposition methods.

The analysis of absorption spectra, excitation spectra, and low-temperature photoluminescence spectra testifies to the formation of new microphases during the growth. The complex spectra can be decomposed into similar structure-constituting spectra shifted against one another on the energy scale. Such spectra are indicators of the formation of new nanophases.

The joint consideration of the photoluminescence spectra, excitement photoluminescence spectra, and absorption spectra testifies to the uniformity of different spectra and the autonomy of each of them. Structurally, the total complexity spectra correlate with the degree of disorder (imperfection) of the crystal and are related to the peculiarities of the defective performance such as a one-dimensional disorder. Three different types of spectra have three different principles of construction and behavior.

Nanostructure-indicator’s spectra are placed on a wide donor–acceptor pair (DAP) spectrum in crystals and films in the case of higher concentrations of non-compensated impurities. The spectra of excitation, photoluminescence spectra and absorption spectra indicate the formation of nanostructures with SiC such as 8H–, 10H–, and 14H–SiC.

In this paper, the D-layers with in-grown disordering in  $\alpha$ -SiC crystals and films (mainly 6H–SiC) and zones of the  $\beta \rightarrow \alpha$  solid phase transformation are investigated. Low-temperature photoluminescence (LTPL) spectroscopy was used as an accurate method highly sensitive to the structure changes.<sup>1–3</sup>

## 2. Experiment

LTPL spectra were registered by a DFS-12 spectrograph with a photodetector (FEU-79). In photoluminescence experiments, a nitrogen LGI-21 337-nm (3.68 eV) or helium-cadmium LG-70 441.6-nm (2.807 eV) laser, a mercury ultrahigh-pressure lamp SVDSH-1000 with a UV-2 filter, and a xenon lamp DKSSH-1000 were used.

The group of single crystalline  $\alpha$ -SiC crystals grown by using Lely's (Tairov's) method under consideration were divided in three groups:

- (1)  $N_{SF}$  samples (colourless): pure crystals with the impurity concentration of  $N_D - N_A \sim (6 \div 7) \times 10^{16} \text{ cm}^{-3}$ ,  $N_D \sim (7 \div 8) \times 10^{16} \text{ cm}^{-3}$ ,  $N_A < 1 \times 10^{16} \text{ cm}^{-3}$ .
- (2)  $N_{DL}$  samples (doped, light-green): with  $N_D - N_A \sim (2 \div 8) \times 10^{16} \text{ cm}^{-3}$ ,  $N_D \sim (5 \div 8) \times 10^{17} \text{ cm}^{-3}$  and  $N_D - N_A > 3 \times 10^{17} \text{ cm}^{-3}$ ,  $N_D > 1 \times 10^{18} \text{ cm}^{-3}$ .
- (3) Cubic crystals of N? samples of the  $n$ -type with  $N_D \leq 3 \times 10^{17} \text{ cm}^{-3}$  (light yellow). Undoped SiC single crystals with the impurity concentration of  $N_D - N_A \sim (2 \div 8) \times 10^{16} \text{ cm}^{-3}$ ,  $N_A \sim (2 \div 8) \times 10^{17} \text{ cm}^{-3}$  and  $N_D - N_A \sim (1 \div 5) \times 10^{17} \text{ cm}^{-3}$ ,  $N_D \geq 1 \times 10^{18} \text{ cm}^{-3}$  were investigated.

Films were obtained by the sublimation "sandwich" and CVD methods.

## 3. Results and Discussion

Figure 1 shows the LTPL spectra depending to the structural imperfection and the impurity concentration in  $\alpha$ -SiC crystals. Structurally perfect 6H-SiC crystals (or perfect blocks of the crystal, which coherently coalesce with disordering layers) show a typical spectrum of nitrogen-bound exciton complexes (PRS) together with

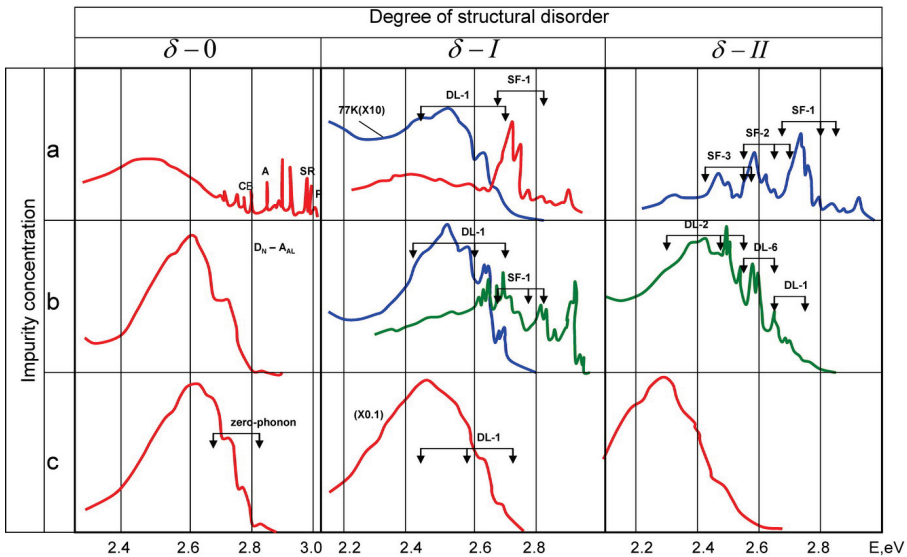


Fig. 1. LTPL spectra according to the structural imperfection and the impurity concentration in  $\alpha$ -SiC crystals.

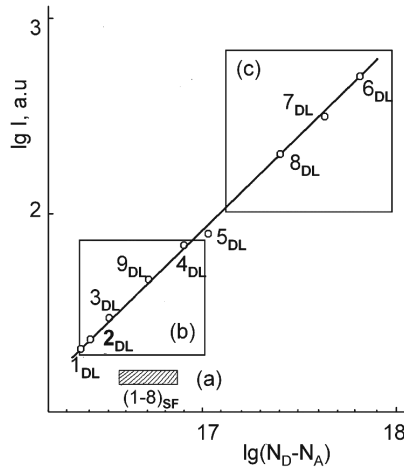


Fig. 2. Intensity of the  $DL_i$  spectra ( $i = 1$ ) ( $T = 77$  K) at  $2.4 \dots 2.5$  V versus the impurity concentration for different samples (of the  $SF_i$  and  $DL_i$  series). Shaded area — the  $SF_i$  spectra from Ref. 6. (a) Most pure samples with only  $SF_i$  spectra,  $N_D - N_A \sim (4 \dots 9) \times 10^{16} \text{ cm}^{-3}$ ,  $(1 \dots 5) \times 10^{16} \text{ cm}^{-3}$ ,  $N_D < 1 \times 10^{17} \text{ cm}^{-3}$ ,  $N_A \sim (1 \dots 3) \times 10^{16} \text{ cm}^{-3}$  from.<sup>6</sup> (b) Pure samples with the  $SF_i$  and  $DL_i$  series,  $N_D - N_A \sim (2 \dots 8) \times 10^{16} \text{ cm}^{-3}$ ,  $N_A \sim (2 \dots 8) \times 10^{17} \text{ cm}^{-3}$ . (c) Samples with only  $DL_i$  spectra,  $N_D - N_A \sim (2 \dots 7) \times 10^{17} \text{ cm}^{-3}$ ,  $N_D < 1 \times 10^{18} \text{ cm}^{-3}$ .

the linear ABC-spectrum related to the Ti  $[(\delta - 0) - (a)]$ , as well as the emission spectra of DAPs.

Here, typical are the spectra  $[(\delta - I) - (a)]$ ,  $[(\delta - II) - (a)]$  of NSF samples,<sup>4-6</sup> as well as  $[(\delta - I) - (b)]$ ,  $[(\delta - II) - (b)]$  of  $N_{DL}$  samples.<sup>7,8</sup>

The peculiarity of the photoluminescence spectra related to the disorder zone depends to a great extent on the impurity concentration in the matrix as the whole. In the pure samples  $N_{SF}$  (case (a)) $_{i=1,2,3}$ , the  $SF_i$  spectra are dominant at a low temperature, whereas the intensity of the  $DL_i$  spectra is very low. On the contrary, the  $DL_i$  spectra are dominant in the doped samples and are located on a broad emission band of DAPs, while the  $SF_i$  spectra are practically invisible.

Peculiarities of the Laue patterns of the D-layers in 6H-SiC crystals are the same as those for 3C-SiC crystals after the phase transformation. The dependence of the intensity of the  $DL_i$  spectra on the impurity concentration is shown in Fig. 2.

Absorption spectra of DL samples are shown in Fig. 3. It can be seen that the absorption is spread far to the lower energy region relative to  $E_{gx}^{6H}$  (exciton band gap in 6H structure). This can be the evidence of the formation of structures with a higher percentage of cubic  $\alpha$ -SiC than 6H-SiC.

The general pattern of the PL spectra of the samples consists of a certain set of the  $SF$  spectra with different intensities. Sometimes, it is peculiar to the different parts of the same crystal. It is shown that all  $SF$  spectra have the identical character, which depends on the structure and is independent of the position on the energy scale.

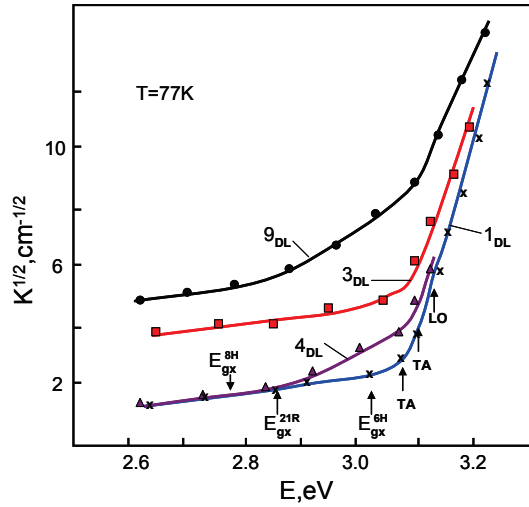


Fig. 3. Absorption spectra of DL samples.

The decoding of the SF-spectrum (as an example, the most typical SF<sub>1</sub> spectrum) shows that its total structure can be obtained by the additive summation of the phonon replica of some zero-phonon parts. In this case, the phonons of the edge of the extended Brillouin zone of SiC (T — 46 meV, LA — 77 meV, TO — 95 meV, LO — 104 meV) are involved.

While the zero-phonon part itself is not detected, it can be “redesigned” according to the structure of the TA replica and transferred as the whole by the TA phonon energy equal to 46 meV to the high-energy region.

The thin linear structure and its readability in the case of different D-layers are different. The minimum half-width of this structure is about 1.5 meV. After the determination of the position of the zero-phonon part of the SF<sub>1</sub> spectrum on the energy scale, it appears that the short-wavelength part of the spectrum coincides with the position of the exciton band gap of 21R polytype at  $T = 4.2$  K (2.853 eV).

The investigation of the photoluminescence excitation spectra ( $\eta_i$ ) reveals that each SF<sub>1</sub> spectrum has its own excitation spectrum.<sup>6</sup> This may be the evidence of some kind of autonomy of each of the SF<sub>1</sub> spectra and their independence of the special part of the crystal disorder and explains their different contributions to the total spectra. It is shown that the long-wavelength edge of each  $\eta_i$  spectrum coincides with the short-wavelength edge of the zero-phonon part of the corresponding SF<sub>1</sub> spectrum. For the given sample, the overall excitation spectrum ( $\sum \eta_i$ ) corresponds to a variation of the absorption coefficient of the D-layer.<sup>2</sup>

Consequently, it is possible, by choosing a suitable photon energy of the exciting radiation, to eliminate the shorter wavelengths of the DL<sub>*i*</sub> spectra from the total complex panorama of the spectrum completely, i.e., to resolve it into the independent components (Fig. 4).

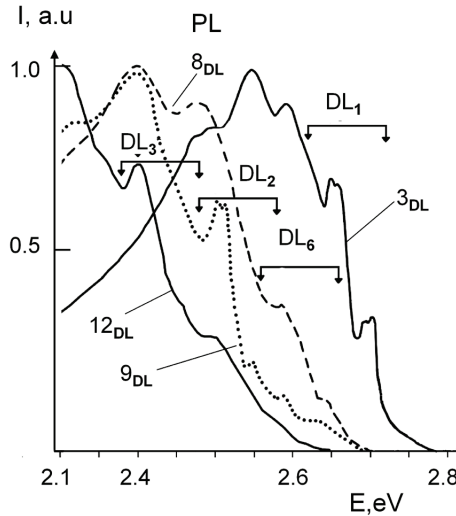


Fig. 4.  $DL_i$  spectra at  $T = 77$  K.

We find that the  $SF_1$  and  $SF_2$  spectra appeared under the excitation with an  $Ar^+$  laser ( $\hbar\nu = 2.54$  eV) and are in the higher energy region. It may be due to the two-photon excitation with the transfer of carriers to the higher energy zones through the intermediate states. The identical character of the  $SF_i$  spectra is backed up by the identical temperature behavior. The peculiarity of this behavior made it possible to decode the thin structure of the spectra.<sup>6</sup>

In view of the positions of the short-wave edges of the zero-phonon part of the  $SF_i$  spectra (2.853, 2.712, 2.611 and 3.002 eV for  $SF_1$ ,  $SF_2$ ,  $SF_3$ ,  $SF_4$  and  $SF_5$ , respectively), as well as the positions of corresponding excitation spectra, we place them on the well-known linear dependence of the exciton gap ( $E_{gx}$ ) on the percentage of hexagonality in different polytypic structures<sup>3,6</sup> (Fig. 5). This gives us a hint concerning the percentage of hexagonality of the new metastable structures appearing in the 6H (33) matrix or in the growth process:

$$\begin{aligned} SF_1 - 14H_1\langle 34 \rangle - 17.5 \text{ \AA} - 28.5\% \text{ (h)}, \\ SF_2 - 10H_2\langle 55 \rangle - 25 \text{ \AA} - 20\%, \\ SF_3 - 14H_2\langle 77 \rangle - 35 \text{ \AA} - 14.3\%. \end{aligned}$$

In several cases, the  $SF_5$  spectra with the motive to build the quasipolytype 33R (3332) – 37% (h) were observed. The formation of the structures  $10H_2\langle 55 \rangle$  and  $14H_2\langle 77 \rangle$  (but not  $10H_1\langle 3223 \rangle - 40\%$  and  $14H_1\langle 4334 \rangle$  (corresponds to  $\langle 34 \rangle$  in 21R)) with the same periods, but with the higher percentages of hexagonality, is backed by the fact that exactly these structures are characterized by the percentage of hexagonality, at which the correspondent values of  $E_{gx}$  are pointed.

The motive of the construction  $\langle 3223 \rangle$  (40% h) of a structure on the metastable microlevel corresponds to the motive of the 15R polytype construction, which occurs

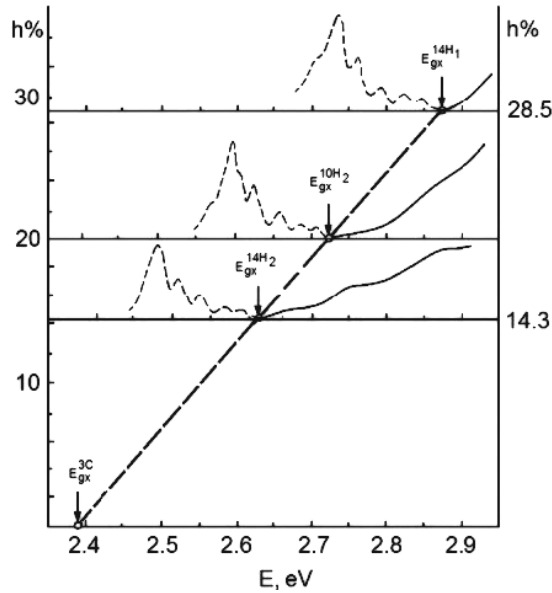


Fig. 5.  $SF_i$  spectrum allocation with respect to the linear dependence of the exciton gap ( $E_{gx}$ ) on the percentage of hexagonality for different polytypic structures. The long-wavelength edges of the excitation spectra are shown. The edges of excitation spectra coincide with the short-wavelength edges of  $SF_i$  spectra at the points corresponding to definite values  $E_{gx}$ .

in a stable state. The motive of  $\langle 4334 \rangle$  (28.6% h) corresponds to the well-known stable 21R polytype.

The low-temperature photoluminescence spectra of pure (Al, N)  $\alpha$ -SiC crystals and pure  $\beta$ -SiC crystals (zones of  $\beta \rightarrow \alpha$  solid phase transformations) are represented by the same  $SF_i$  spectra, which are indicators of the intermediate metastable micro- and nanostructures with the medium intermediate percentage of hexagonality regarding 6H and 3C phases, namely, 21R $\langle 34 \rangle$ , 10H $_2\langle 55 \rangle$ , 14H $_2\langle 77 \rangle$ .

In pure SiC crystals, the  $SF_i$  spectra are dominant.<sup>6</sup> In crystals with higher impurity concentrations, the  $DL_i$  spectra appear.

The  $DL_i$ -type spectra are different from the  $SF_i$  spectra and have other principles of construction and behavior. They are located on a broad DAP emission band in crystals with higher concentrations of non-compensated impurities (Fig. 1).

Structurally, the general complexity of the  $DL_i$  spectra correlates with the degree of disorder of the crystal and is related to the one-dimensional disorder, the same as in the case of stacking fault ( $SF_i$ ) spectra.

The analysis of the absorption, excitation and low-temperature photoluminescence spectra suggest the formation of a new microphase during the growth and the appearance of the deep-level (DL) spectra, so that the complex spectra of the crystals can be decomposed into the so-called  $DL_i$  ( $i = 1, 2, 3, 4$ ) spectra. All spectra of the DL type demonstrate the identical behavior of the thin structure. If the  $SF_i$

and  $DL_i$  spectra are reconciled at the long-wavelength part, such combinations of spectra are along the line of the dependence  $E_g = f$  (percentage of hexagonality). Herein, the  $SF_i$  and  $DL_i$  spectra exist independently, and they have different ways to behave themselves. However, they match the same nanostructure transformations at  $\alpha \rightarrow \beta$  and  $\beta \rightarrow \alpha$  transitions.<sup>9-14</sup>

#### 4. Conclusions

The peculiarity of the photoluminescence spectra related to the zones of disorder to a great extent depends on the impurity concentration in the matrix as the whole. In pure samples  $N_{SF}$  (case (a))  $i = 1, 2, 3, \dots$ , the  $SF_i$  spectra are dominant at a low temperature, whereas the intensity of the  $DL_i$  spectra is very low.

On the contrary, the  $DL_i$  spectra are dominant in the doped samples and are located on a broad emission band of donor-acceptor pairs, while the  $SF_i$  spectra are practically invisible.

In view of the positions of the short-wave edges of the zero-phonon part of the  $SF_i$  spectra, as well as the positions of corresponding excitation spectra, we place them on the well-known linear dependence of the exciton gap ( $E_{gx}$ ) on the percentage of hexagonality in different polytypic structures, which gives a hint concerning the percentage of hexagonality of the new metastable structures appearing in the 6H (33) matrix or in the growth process. The SF spectra are indicators of the appearance of such metastable structures.

#### References

1. F. Yan, dissertation Low Temperature Study of Defect Centers in Silicon Carbide, University of Pittsburgh, 2009. pp. 153. (Dissertation LTPL-Choyke Pittsburgh 2009, etd-08052009-012630).
2. I. S. Gorban and G. N. Mishinova, *Proc. SPIE* **3359**, 187 (1998).
3. W. J. Choyke, H. Matsunami and G. Pensl, *Silicon Carbide: Recent Major Advances* (Berlin, Springer, 2004) (October 8, 2003), p. 68.
4. S. I. Vlaskina et al., *Semiconduct. Phys. Quant. Electron. Optoelectron.* **14**(4), 432 (2011).
5. S. I. Vlaskina et al., *Semiconduct. Phys. Quant. Electron. Optoelectron.* **16**(2), 132 (2013).
6. S. I. Vlaskina et al., *Semiconduct. Phys. Quant. Electron. Optoelectron.* **16**(3), 272 (2013).
7. S. I. Vlaskina and D. H. Shin, *Jpn. J. Appl. Phys.* **38**, 27 (1999).
8. S. W. Lee et al., *Semiconduct. Phys. Quant. Electron. Optoelectron.* **13**(1), 24 (2010).
9. S. Shinozaki and K. R. Kisman, *Acta Metallurgica* **26**, 769 (1978).
10. L. U. Ogbuji, T. E. Mitchell and A. H. Heuer, *J. Amer. Ceram. Soc.* **64**(2), 91 (1981).
11. K. Kobayashi and S. Komatsu, *J. Phys. Soc. Jpn. Appl.* **81**(2), 024714 (2012).
12. A. V. Soldatov, N. N. Bogolyubov Jr. and S. P. Kruchinin, *Quantum Matter* **6**, 21 (2014).
13. S. Kruchinin and T. Pruschke, *Phys. Lett. A* **378**, 157 (2014).
14. V. E. Rodionov et al., *Mater. Sci.* **31**, 232 (2013).